

Periodic Trends in the Character of First-Row Transition Metals-Based Catalysts Embedded on Mordenite

Khoirina Dwi Nugrahaningtyas^{(a)*}, Mitha Fitria Kurniawati^(a), Abu Masykur^(a), Nisriina 'Abidah Quratul'aini^(b)

^(a) Department of Chemistry, Faculty of Mathematic and Natural Science, Sebelas Maret University, Jl. Ir. Sutami No 36 A, Kentingan, Surakarta, Jawa Tengah, Indonesia

^(b) Department of Chemical Engineering, Faculty of Engineering, Sebelas Maret University, Jl. Ir. Sutami No 36 A, Kentingan, Surakarta, Jawa Tengah, Indonesia

Abstract

This research studied the effect of transition metals (TMs) in one period (TMs = Fe, Co, Ni, Cu, and Ag) on the characteristics of mordenite zeolite. The loading method used was wet impregnation with 0.025 M metal salt concentrate. The results showed that TMs could be impregnated on mordenite, which was indicated by a shift in the wavelength of certain functional groups. However, the metal loading did not cause a change in the diffraction pattern of mordenite. The periodicity of transition metals impacts the strength of acidity and texture of the catalyst, where the optimum strength of acidity, surface area, pore-volume, and average pore radius is Co/Mor. Morphological analysis showed that TMs/mordenite catalyst was more heterogeneous than mordenite.

* Corresponding author:

khoirina@mipa.uns.ac.id

Received 12 April 2022

Revised 28 April 2022

Accepted 27 May 2022

Keywords: Catalyst, first-row transition metals, mordenite, periodic trends.

1. Introduction

Due to economic growth and population, the energy crisis has forced the petroleum industry to process low-quality oil sources, which can be improved using a catalytic process. The catalytic process also can reduce energy requirements and emissions that cause air pollution[1]. Zeolite-based catalysts usually use in the petroleum industry. However, modifications must be made, such as adding a metal as the catalyst active site to obtain a metal-supported catalytic system with high catalytic activity[2], [3]. Metal-supported catalytic systems can prepare by several methods such as ion exchange, coprecipitation, and impregnation. Sakizci and coworkers synthesized a metal-supported catalytic system, namely Fe, Cu, and Ag, loaded on mordenite using the ion exchange method[4]. The result showed that the peak characteristics of mordenite did not change, but there was a decrease in the surface area of mordenite after the metal loading. Li and coworkers modified Al_2O_3 catalyst with Ni metal using the coprecipitation method [5]. They found that the catalysts contain a NiAl_2O_4 phase which is difficult to reduce because the Ni metal is tightly bound to Al_2O_3 . While, Nugrahaningtyas and friends (2009) modified the USY catalyst with Ni metal using the impregnation method[6]. They obtained that the addition of Ni metal to the USY catalyst produced Ni and NiO phases and increased the acidity of the catalyst. Catalyst preparation is influenced by, among others, time, temperature, metal precursor and concentration[7]–[10]. Sakizci and coworkers, who prepared mordenite supported by Fe, Cu, and Ag through a reflux process at 80 °C, found a decrease in surface area [4]. Ulla and colleagues prepared Co/mordenite catalyst with a reflux process at room temperature of 30 °C for 16 hours, then raised to 80 °C for 4 hours at a pressure of 1 atm with a concentration of 0.025 M precursor metal[8]. They found that the metals had evenly distributed but in the form of metal ions. Majdan and colleagues modified mordenite with metals Mn, Co, Ni, Cu, Zn, and Cd and found that the ions such as Mn^{2+} , Co^{2+} , Cu^{2+} , and Zn^{2+} underwent cation exchange with protons at the Brønsted acid site to produce an inner sphere complex[11]. Meanwhile, Ni^{2+} and Cd^{2+} ions were associated with the Brønsted acid site without undergoing cation exchange. Another researches also modified mordenite with different metals, namely Fe, Co, Ni, Cu, and Zn[12]. They found that the catalysts had better activity and selectivity than mordenite. However, the metals were supported in metal ions form and decreased in acidity. Meanwhile, CoMo/Mordenite catalyst has acidity and demethoxy anisol activity 150 and 122 times higher, respectively, than mordenite[13]. The increased acidity has thought due to the ammonia addition in the catalyst synthesis process, which blocks the Brønsted acid site and prevents the cations exchange with Co or Mo. In addition, catalyst activation in the form of calcination and reduction has also proven to succeed in reducing Co and Mo metals into their metallic elements capable of donating Lewis acid sites. The previous studies indicate that the preparation method, the type of metal, and the carrier will impact the characteristics, including the activity of the catalyst. Somehow, there has been no research on the periodicity of the metal on the features of a catalyst. Therefore, this study investigates the effect of adding the metals from one period and one group on phase composition, the intensity of peak characteristics, functional groups, acidity, surface area, and morphology of mordenite.

2. Experimental

2.1. Materials

Synthetic H-Mordenite (HS-690, Powder) was purchased from Wako. Iron (III) nitrate nonahydrate, Cobalt(II) nitrate hexahydrate, Nickel(II) nitrate hexahydrate, Copper(II) nitrate trihydrate, Zinc(II) nitrate tetrahydrate, and Silver nitrate were purchased from Sigma Aldrich. Meanwhile, N_2 and H_2 gases were obtained from SAMATOR without purification.

2.2. Preparation of TMs/MOR Catalyst

Several grams of mordenite were immersed in ammonia (25% pa), that followed by the addition of nonahydrate Iron (III) nitrate and double distilled water. The solution refluxed at 30 °C for 16 hours then, the temperature was increased up to 80°C and kept for 4 hours, then filtered. The residue evaporated using a rotary evaporator to become a powder. Next, the sample was calcined at a temperature of 550 °C for 3 hours with N₂ gas. In the next step, the sample was reduced at 400 °C for 2 hours with H₂ gas. The dry powder obtained called Fe/Mordenite was then stored in a desiccator. The same procedure was repeated for various metal salts types, such as Cobalt (II) nitrate hexahydrate, Nickel (II) nitrate hexahydrate, Copper (II) nitrate trihydrate, Zink (II) nitrate tetrahydrate, and silver nitrate, until obtained Co/Mordenite, Ni/Mordenite, Cu/Mordenite, Zn/Mordenite, and Ag/Mordenite, respectively.

2.3. Catalyst Characterization

All the catalysts characterized for their metal content using X-ray fluorescence spectrometry (BRUKER S2 Ranger). The acidity of the catalyst was analyzed qualitatively using an ammonia-based molecular probe according to the procedure in our previous study[13], [14]. The analysis of crystallinity, functional groups, and catalyst morphology followed previous methods [15], [16]. The supporting metal phases were detected using the Le bail method with Rietica software. Meanwhile, the particle size distribution in the sample was measured using measureIT software.

3. Results and discussion

3.1. Metal Contents

The effect of the addition of transition metals on Si and Al contained in mordenite was analyzed using XRF (X-Ray Fluorescence) (Figure 1a). Figure 1a shows that the Si/Al ratio of the metal-impregnated mordenite catalyst tend to decreased. The decrease in the Si/Al ratio may be due to the dissolved silica during alkali treatment [17]. However, in this study, the Si/Al ratio decreased is no significant, indicating that the silica dissolution process did not occur. The study results in good agreement with Sakizci and coworkers that the Si/Al ratio of Cu/Mordenite, Fe/Mordenite, and Ag/Mordenite decreased due to the presence of metals[4].

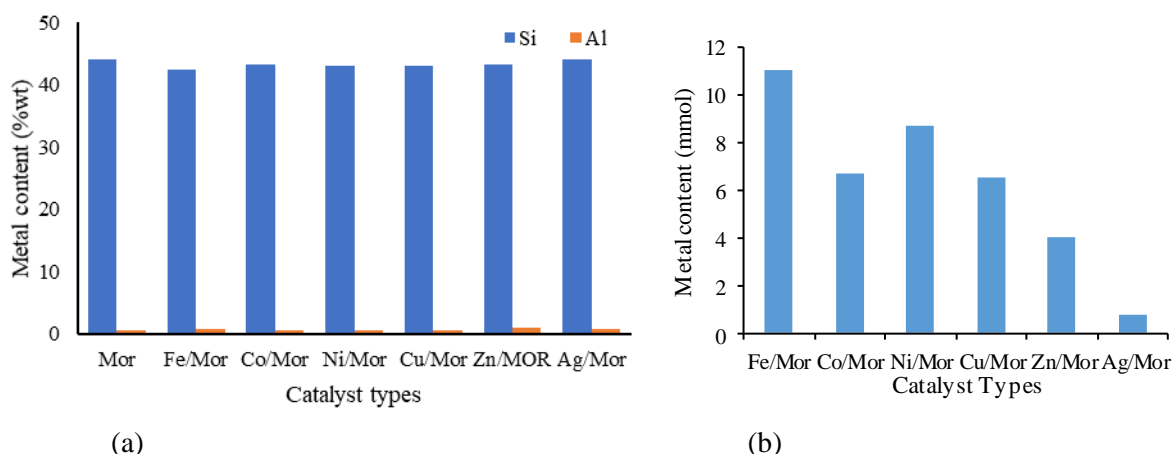


Figure 1. The metals content of catalysts viz. (a) The Si and Al content and (b) Transition metal (TMs).

Furthermore, metal content analysis carried out using XRF on the mordenite catalysts impregnated with transition metals (Fe, Co, Ni, Cu, and Ag) (Fig 1b). Figure 1b shows that the TMs (Fe, Co, Ni, Cu, and Ag) successfully impregnated in mordenite. Iron was the most impregnated metal because of its relatively smaller size, compared with

others. The increase of Fe content in the catalyst is directly proportional to the amount of Fe metal added to mordenite, not for other TMs.

3.2. Diffraction Pattern Analysis

Analysis of the diffraction pattern, type of phase, and crystal structure carried out to determine the effect of metal addition on the crystal structure of mordenite (Figure 2).

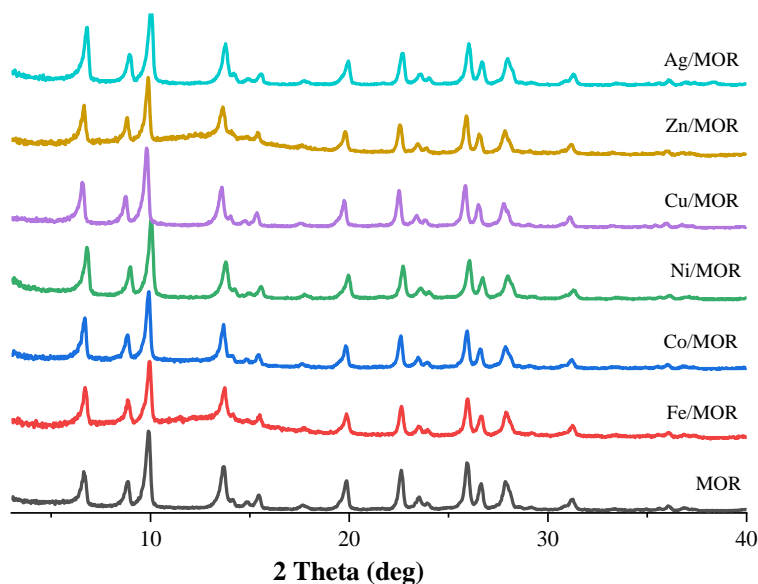


Figure 2. Diffraction patterns of mordenite and TMs/mordenite.

Figure 2 shows the mordenite characteristic peaks at 2θ ($^{\circ}$) = 9.8° , 13.66° , 19.8° , 22.62° , and 25.9° , according to ICSD standards #4393 and #4394. Based on the diffractogram pattern analysis of each catalyst, it was found that metal loading did not effect on the mordenite's crystallinity. However, there was a decrease in intensity at $2\theta = 15.23^{\circ}$; 19.57° , and 25.67° for Fe/MOR and Zn/MOR, associated with composition changes due to cation exchange[4].

The next analysis was refinement with Le Bail method using RIETICA software. The results showed that the mordenite sample used complied with the two mordenite standards (Figure 3). The first suitable standard was ICSD #4393 and ICSD #4394.

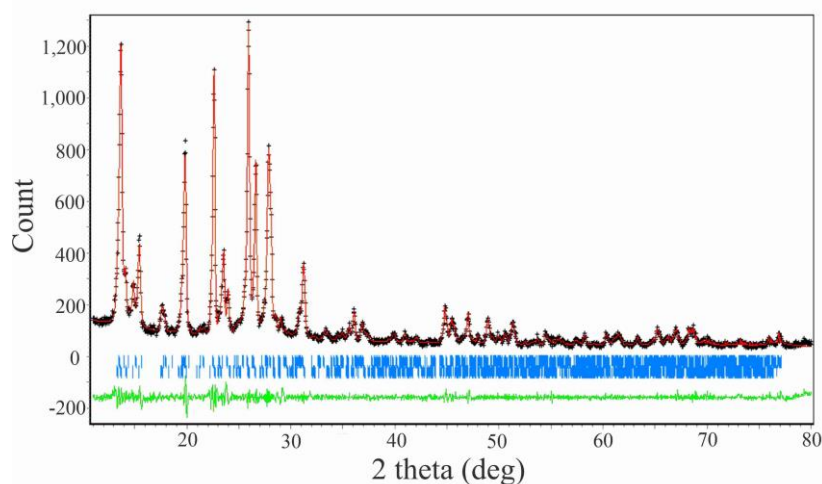


Figure 3. Le Bail plot of mordenite X-ray diffraction data with two mordenite standards (ICSD #4393 and ICSD #4394). Experimental data (+); calculation result (---); experimental data vs calculation results (---).

The next analysis was the refinement of all catalysts with ICSD #4393 standards. It was found that the addition of different metals did not change the crystal structure or the spatial group of mordenite (Table 1). However, the addition of different types of transition metals led to an increase in cell parameters *a*, *b*, and *c* that were different. The increase in lattice parameters was possibly due to the presence of metal inserting in the pores of mordenite so that the cell volume of TMs/mordenite also increased.

Table 1. Refinement results using mordenite standards ICSD #4393.

Parameter Sel	Mordenite	Fe/Mor	Co/Mor	Ni/Mor	Cu/Mor	Zn/Mor	Ag/Mor
<i>a</i> (Å)	17.65	18.34	18.12	18.09	17.80	17.82	18.01
<i>b</i> (Å)	19.75	20.44	20.16	20.58	20.03	19.89	20.33
<i>c</i> (Å)	7.26	7.54	7.54	7.55	7.42	7.35	7.49
Cell Volume (Å ³)	2528.8	2827.5	2724	2812.3	2646.5	2602.4	2742.4

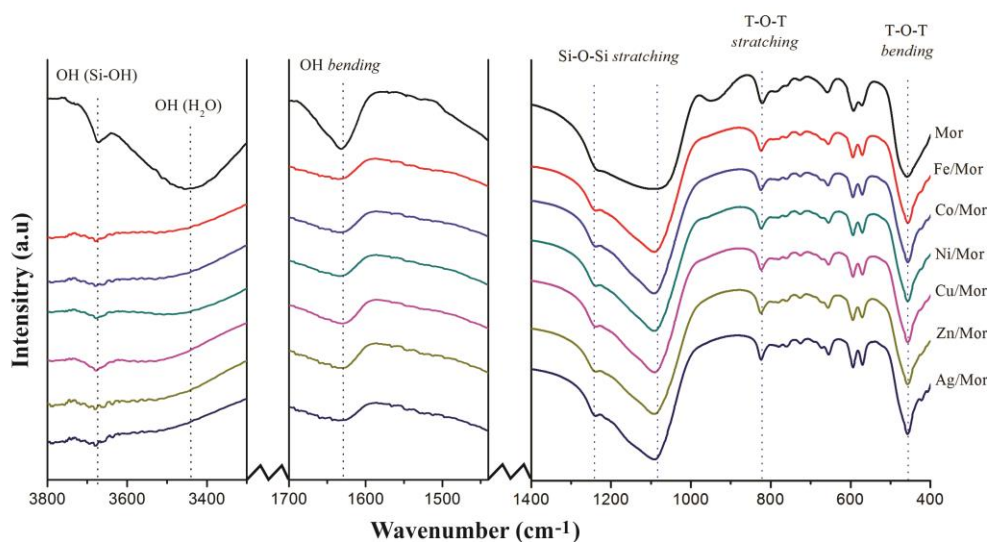
The addition of one-period transition metals to mordenite shows the periodicity of the properties. In one period, from left to right, the cell volume decreases; and within a group, from top to bottom, the cell volume increases. These properties correspond to the periodicity of the size of each metal element on the periodic table. These strengthen the notion that the transition metals loaded successfully inserted between the pores of the mordenite. The same results were also obtained in the refinement using the ICSD #4394 standard. Further analysis using the Le Bail method was carried out to determine the metal phase present in the catalyst. The phase standard data and the percentage of the molar weight presented in Table 2. The phases of the metal loaded on the TMs/mordenite catalyst were pure metal and metal oxide (Table 2). There are also find that the most amount metal in mordenite was Co (Table 2), while XRF data showed it was Fe (Fig. 1b). This fact indicates that Co is more exposed to the surface of mordenite compared to other metals. This phenomenon also occurred to Ag; the XRF data showed that Ag slightly trapped in mordenite (Fig. 1b), but the XRD analysis results showed it relatively large than other metals (Table 2). Further analysis of the functional groups of each catalyst uses to prove the effect of adding various types of transition metals to the mordenite surface.

Table 2. Data of standard and molar weight (%) of each phase

Phase	Molar Weight (%)					
	Mordenite	Fe/Mor	Co/Mor	Ni/Mor	Cu/Mor	Ag/Mor
Mordenite (#4393)	48.59	48.54	48.34	49.49	48.44	48.85
Mordenite (#4394)	51.41	49.52	49.18	50.28	50.12	50.66
Element		0.06 (Fe)	0.06(Co)	0,06(Ni)	0.07(Cu)	0,10(Ag)
Oxide-1		0.12(FeO)	0.03(CoO)	0.06(NiO)	0.11(CuO)	0.16(AgO)
Oxide-2			0.61(CoO ₂)	0.11(NiO ₂)	1.21(CuO ₂)	
Oxide-3			0.23(CoO ₃)		0.06(Cu ₂ O)	0.09(Ag ₂ O ₃)
Oxide-4		1.76(Fe ₃ O ₄)	1.55(Co ₃ O)			0.14(Ag ₃ O ₄)

3.3. Functional Groups

Analysis of the functional groups on the catalyst showed the four absorption types that corresponded to the OH group (Figure 4). The first absorption type found in the wavenumber of 3678-3680 cm^{-1} , which thought to come from the absorption of the silanol group(Si-OH). The second absorption type found in the wavenumber of 3446-3509 cm^{-1} corresponds to the absorption of the OH stretching functional group from water molecules adsorbed on the surface. The third absorption-type in the wavenumber of 1629-1636 cm^{-1} was possible from the OH bending group[18]. Meanwhile, the fourth absorption in the wavenumber region of 3209 cm^{-1} was possible from the OH group of the absorbed water.

**Figure 4.** FTIR spectra on mordenite and TMs/Mordenite.

The absorption in the wavenumber of 1057-1096 cm^{-1} was possible from the internal Si-O-Si vibration connected to the Si-O(Al) vibration[19]. The absorption in the wavenumber of 909 cm^{-1} indicated the presence of Al-O-Al bending absorption[12]. The absorptions in the wavenumber of 820-827 cm^{-1} and 454-464 cm^{-1} were Si(Al)-O stretching and Si(Al)-O bending vibrations [20]. The transition metal is bonded to mordenite by covalent coordination. It causes a shift in the characteristic adsorption wavenumber of mordenite. The wavenumber is equivalent to the binding energy of a functional group. If the wavenumber is shifting to the right, then the binding energy of a functional group is getting weaker, and vice versa. The wavenumber of mordenite in the Si (Al)-O stretching was 820 cm^{-1} . However, the wavenumber tends to the left after the addition of metal. It indicated that the functional group has a strong bond.

Meanwhile, the wavenumber of mordenite in the Si (Al)-O bending was 464 cm^{-1} and tended to the right after metal loaded. So it is indicated that the addition of metal causes the bond in the functional group to become weak. The silanol (Si-OH) and Si-O-Si absorption tended to the left, while the Si-OH-Al and OH bending absorption tend to the right. On the other hand, the decrease in O-H adsorption intensity might be due to some H^+ cations at the Brønsted acid site of mordenite was replaced by metals. In general, the addition of metal did not cause a shift in the absorption of functional groups from mordenite. That is presumably because the functional groups have a stable bond. However, it found that the wavenumber absorption of 3209 cm^{-1} disappeared after the addition of metal, which had thought to be due to the replacement of H^+ cations by metals and the formation of OM groups[12]. Disappear of absorption on 947 cm^{-1} is thought to be due to the release of Si^{4+} after treatment with an ammonia base. In one period (Fe, Co, Ni, and Cu) from left to right, we found that the wavenumbers for several functional groups are getting bigger (Figure 4). It indicated that the binding energy of the functional groups is getting bigger, too. While, in one group (Cu and Ag), from top to bottom, the wavenumber of the functional groups get smaller, indicating that the binding energy of the functional groups is getting smaller. The results also showed that the addition of TMs did not cause a change in the absorption of functional groups in mordenite. However, the functional group's analysis cannot use for active site analysis. One of the essential active sites in the hydrotreatment reaction is the Brønsted and Lewis acid sites. Therefore, the next step in this research is to determine the acidity qualitatively.

3.4. Acidity Properties

Mordenite has three types of Brønsted acid sites associated with OH absorption regions at different frequencies. The first type is a Brønsted acid site originating from a proton bound to the great cavity of mordenite (ring 12), which occurs at a high frequency equivalent to the wavenumber 3678 cm^{-1} . The second type is the form of a Brønsted acid site on ring 8. That is due to the presence of an OH group on the side pocket, which has a small wavenumber (medium-frequency) of 3478 cm^{-1} [21], [22]. Meanwhile, the third type originates from the Brønsted acid site associated with absorption at a wavenumber of 3129 cm^{-1} (low frequency)[22]. In addition to the three types of Brønsted acid sites, modernite also has one type of Lewis acid site, namely at wave number 1402 cm^{-1} [22].

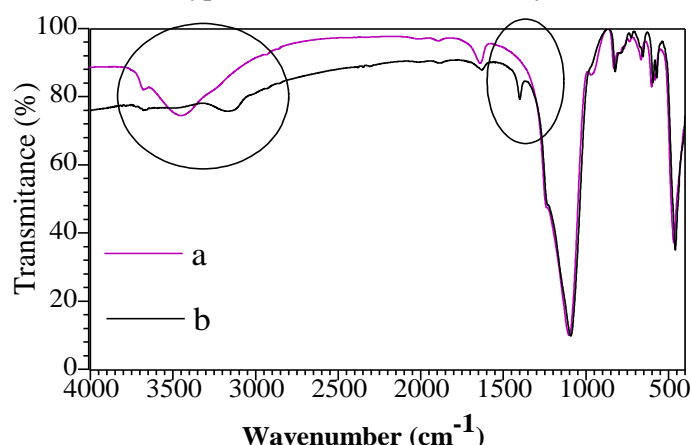


Figure 5. FTIR spectra of mordenite (a) before and (b) after ammonia adsorption.

The presence of Brønsted and Lewis acid sites can be analyzed qualitatively using a molecular probe of an ammonia base and detected by FTIR spectroscopy. The FTIR spectra can show the interaction between the ammonia molecule probe and the acid site on the catalyst surface and predict the bond strength of the Brønsted acid site and the Lewis acid site. The part of the spectra marked with a circle is the location of the bond between the ammonia molecule probe

and the Brønsted acid site, and the Lewis acid site (Figure 5). The absorption shift at the wavenumber of 1402 cm^{-1} indicated an electron transfer from the Lewis acid site to the ammonia molecule as a probe molecule. The absorption in the wavenumber around $3600\text{--}3000\text{ cm}^{-1}$ comes from the interaction between the Brønsted acid site and ammonia to form ammonium ions. At this site, a proton transfer process occurs from the surface of the Brønsted acid site to ammonia, which causes ammonia to be protonated[23]. Metal loading affects the absorption intensity and wavenumber shift of each functional group of mordenite after ammonia adsorption (Figure 6). The intensity of the absorption of Brønsted and Lewis acid sites in Fe/mordenite is the largest compared to other catalysts (Figure 6). The higher the absorption intensity, the higher the amount of ammonia adsorbed. However, the acidity of transition metal-modified mordenite was lower than that of unmodified mordenite. The decrease in acidity intensity was possible due to the substitution of H^+ cations at the Brønsted site and closure of the Lewis site by transition metals[4].

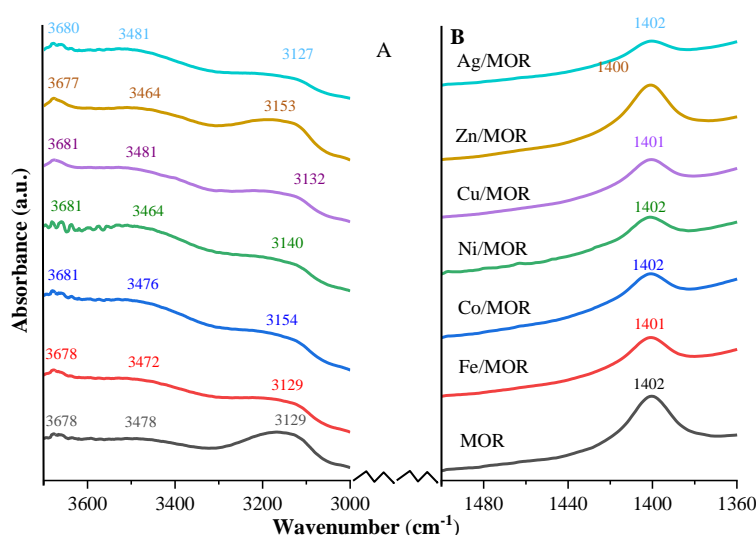


Figure 6. FTIR uptake of mordenite and TMs/mordenite at Brønsted (A) and Lewis (B) sites.

The Brønsted acid sites of all TMs/Mordenite catalysts tended to shift to the left compared to mordenite. Meanwhile, the absorption wavenumber of the Lewis acid site is constant. It indicated that the Brønsted acidity of the TM/mordenite catalyst is stronger than mordenite. Based on the FTIR spectrum, we can perform a qualitative analysis of the catalyst acidity. Here, we found that the addition of transition metals can increase the acidity strength periodically. The addition of transition metals in one period (Fe, Co, Ni, and Cu), from left to right, increased the acid strength, while in one group (Cu and Ag), from top to bottom, reduced the acidity. The effect of transition metals loading on the structure of mordenite was analyzed further by the surface area, average pore radius, and pore volume of the catalyst.

3.5. Surface Area, Average Pore Radius, and Total Pore Volume

Analysis of the surface area of the catalysts showed a decrease in the surface area of mordenite after the addition of transition metals (Figure 7). The reduction of the surface area due to uneven metal dispersion, causing metal accumulation and partially covering the mordenite pores[4]. Meanwhile, the large surface area of Co/mordenite catalyst indicates that Co was evenly dispersed compared to other metals. The addition of transition metals of one period from left to right (Fe, Co, Ni, and Cu) caused the surface area to decrease, so did the addition of those in one group, from top to bottom (Cu and Ag). These phenomena were due to different metal particle sizes. The large metal particle size tended to cover the surface of the mordenite so that the surface area decreased. The presence of metal

loaded on mordenite also caused the average value of the pore radius and pore volume of mordenite to tend to increase. The smaller the surface area, the larger the average pore radius because the average pore radius was inversely proportional to the specific surface area[24].

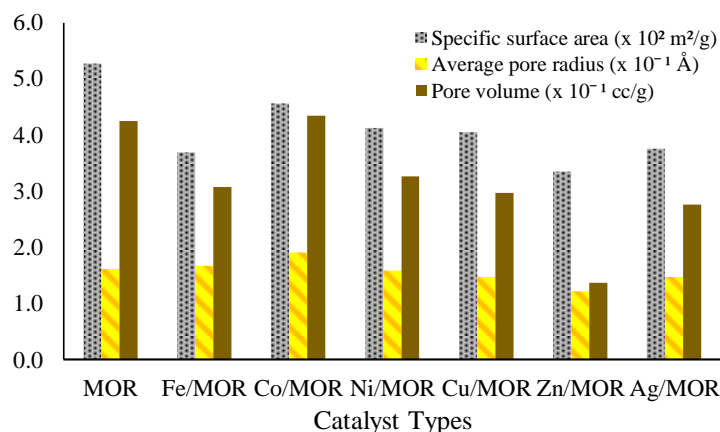


Figure 7. The relationship of Mor and TMs/Mor topology: (A) Surface area, (B) Average pore radius and (C) Pore volume.

3.6. Analysis of Morphology

The morphological analysis showed that mordenite and TMs/mordenite had different particle sizes and shapes. Mordenite has a homogeneous crystal arrangement, while the TMs/Mordenite catalyst has a heterogeneous crystal arrangement. Not all of the metals can be seen visually on the mordenite surface. Overall, their morphologies still look similar to the morphology of mordenite, which is like a needle (Figure 8)[12]. Based on the refinement of the XRD data, the crystal lattice parameters experienced insignificant changes so that it was possible for the metals loaded to have a small size. It shows that the metals were dispersed in small sizes and did not form a bulk. Based on the characteristics of the TMs/mordenite catalysts above, mordenite can disperse transition metals (Fe, Co, Ni, Cu, and Ag) on its surface.

4. Conclusion

The transition metals (TMs = Fe, Co, Ni, Cu, and Ag) can be impregnated on mordenite, as evidenced by the presence of these metals in mordenite. The transition metals loading caused: a change of phase composition, a shift of functional group wavenumber, morphology, a decrease in the intensity of the characteristic peaks of mordenite, acidity, and surface area. The addition of metals in one period (Fe, Co, Ni, and Cu) from left to right further increases the strength of the acidity, while those in one group (Cu and Ag) from top to bottom weakened.

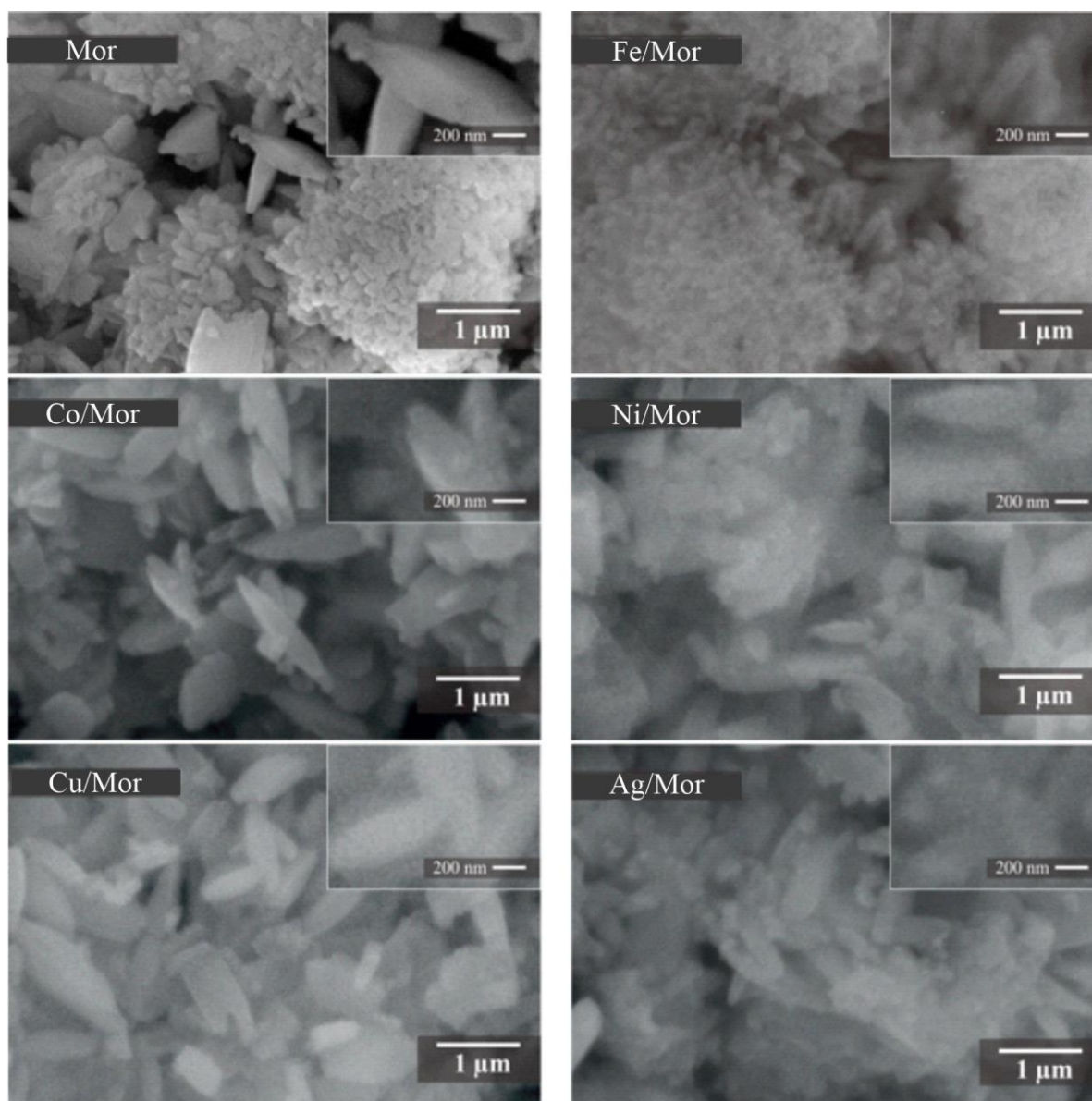


Figure 8. The morphology of mordenite and TMs/mordenite.

Acknowledgments

Authors thank to The Directorate General of Research and Community Service (DP2M DIKTI) for funding this research through HIBAH PENELITIAN DASAR 2021.

References

- [1] Z. Y. Jing *et al.*, “Nickel catalysts on hydrodeoxygenation of fatty acid methyl esters to fuel-like hydrocarbons,” *Ranliao Huaxue Xuebao/Journal Fuel Chem. Technol.*, vol. 46, no. 4, pp. 427–440, Apr. 2018, doi: 10.1016/S1872-5813(18)30018-5.
- [2] J. Zhang, B. Fidalgo, A. Kolios, D. Shen, and S. Gu, “Mechanism of deoxygenation in anisole decomposition over single-metal loaded HZSM-5: Experimental study,” *Chem. Eng. J.*, vol. 336, pp. 211–222, Mar. 2018, doi: 10.1016/j.cej.2017.11.128.
- [3] Y. Xu *et al.*, “Effect of iron loading on acidity and performance of Fe/HZSM-5 catalyst for direct synthesis of aromatics from syngas,” *Fuel*, vol. 228, no. January, pp. 1–9, 2018, doi: 10.1016/j.fuel.2018.04.151.

- [4] M. Sakizci and L. Özgül Tanriverdi, "Influence of acid and heavy metal cation exchange treatments on methane adsorption properties of mordenite," *Turkish J. Chem.*, vol. 39, no. 5, pp. 970–983, 2015, doi: 10.3906/kim-1501-71.
- [5] G. Li, L. Hu, and J. M. Hill, "Comparison of reducibility and stability of alumina-supported Ni catalysts prepared by impregnation and co-precipitation," *Appl. Catal. A Gen.*, vol. 301, no. 1, pp. 16–24, 2006, doi: 10.1016/j.apcata.2005.11.013.
- [6] K. . D. Nugrahaningtyas, W. Trisunaryanti, D. M. Widjonarko, A. Yusnani, D. M. Widjonarko, and A. Yusnani, "Preparation and Characterization The Non-Sulfided Metal catalyst: Ni/USY and NiMo/USY," *Indo. J. Chem.*, vol. 9, no. 2, pp. 177–183, 2009, doi: 10.22146/ijc.21526.
- [7] L. Wei *et al.*, "Influence of nickel precursors on the properties and performance of Ni impregnated zeolite 5A and 13X catalysts in CO₂ methanation," *Catal. Today*, no. May, pp. 0–1, 2020, doi: 10.1016/j.cattod.2020.05.025.
- [8] M. A. Ulla *et al.*, "Preparation and characterization of Co mordenite coatings onto cordierite monoliths as structured catalysts," *Catal. Today*, vol. 133–135, no. 1–4, pp. 42–48, 2008, doi: 10.1016/j.cattod.2007.11.052.
- [9] P. L. Tan, C. T. Au, and S. Y. Lai, "Effects of acidification and basification of impregnating solution on the performance of Mo/HZSM-5 in methane aromatization," *Appl. Catal. A Gen.*, vol. 324, no. 1–2, pp. 36–41, 2007, doi: 10.1016/j.apcata.2007.03.002.
- [10] P. Tan, "Ammonia-basified 10 wt% Mo/HZSM-5 material with enhanced dispersion of Mo and performance for catalytic aromatization of methane," *Appl. Catal. A Gen.*, vol. 580, no. January, pp. 111–120, 2019, doi: 10.1016/j.apcata.2019.05.011.
- [11] M. Majdan, M. Kowalska-Ternes, S. Pikus, P. Staszczuk, H. Skrzypek, and E. Zięba, "Vibrational and scanning electron microscopy study of the mordenite modified by Mn, Co, Ni, Cu, Zn and Cd," *J. Mol. Struct.*, vol. 649, no. 3, pp. 279–285, Apr. 2003, doi: 10.1016/S0022-2860(03)00082-6.
- [12] S. S. Priya, P. R. Selvakannan, K. V. R. Chary, M. L. Kantam, and S. K. Bhargava, "Solvent-free microwave-assisted synthesis of solketal from glycerol using transition metal ions promoted mordenite solid acid catalysts," *Mol. Catal.*, vol. 434, pp. 184–193, 2017, doi: 10.1016/j.mcat.2017.03.001.
- [13] K. D. Nugrahaningtyas, N. Rahmawati, F. Rahmawati, and Y. Hidayat, "Synthesis And Characterization Of CoMo/Mordenite Catalyst For Hydrotreatment Of Lignin Compound Models," *Open Chem.*, vol. 17, no. 1, pp. 1061–1070, Dec. 2019, doi: 10.1515/chem-2019-0120.
- [14] K. D. Nugrahaningtyas, E. Herald, Rachmadani, Y. Hidayat, and I. Kartini, "Effect of synthesis and activation methods on the character of CoMo/ultrastable Y-zeolite catalysts," *Open Chem.*, vol. 19, no. 1, pp. 745–754, Jun. 2021, doi: 10.1515/chem-2021-0064.
- [15] K. D. Nugrahaningtyas, I. F. Nurcahyo, and M. Zulkarnain, "Characterization of metal oxide and morphology of CuMo/mordenite," *AIP Conf. Proc.*, vol. 2243, no. June, pp. 5–6, 2020, doi: 10.1063/5.0002525.
- [16] K. D. Nugrahaningtyas, M. M. Putri, and T. E. Saraswati, "Metal phase and electron density of transition metal/HZSM-5," in *AIP Conference Proceedings*, 2020, vol. 2237, no. June, p. 020003, doi: 10.1063/5.0005561.
- [17] G. Jozefaciuk and G. Bowanko, "Effect of acid and alkali treatments on surface areas and adsorption energies of selected minerals," *Clays Clay Miner.*, vol. 50, no. 6, pp. 771–783, 2002, doi: 10.1346/000986002762090308.
- [18] S. Yang *et al.*, "Determination of Ni(II) uptake mechanisms on mordenite surfaces: A combined macroscopic and microscopic approach," *Geochim. Cosmochim. Acta*, vol. 75, no. 21, pp. 6520–6534, 2011, doi: 10.1016/j.gca.2011.08.024.
- [19] O. Korkuna, R. Lebeda, J. Skubiszewska-Zięba, T. Vrublevs'ka, V. M. Gun'ko, and J. Ryczkowski, "Structural and physicochemical properties of natural zeolites: Clinoptilolite and mordenite," *Microporous Mesoporous Mater.*, vol. 87, no. 3, pp. 243–254, Jan. 2006, doi: 10.1016/j.micromeso.2005.08.002.

- [20] N. Mansouri, N. Rikhtegar, H. Ahmad Panahi, F. Atabi, and B. K. Shahraki, "Porosity, characterization and structural properties of natural zeolite - Clinoptilolite - As a sorbent," *Environ. Prot. Eng.*, vol. 39, no. 1, pp. 139–152, 2013, doi: 10.5277/EPE130111.
- [21] D. B. Lukyanov, T. Vazhnova, N. Cherkasov, J. L. Casci, and J. J. Birtill, "Insights into Brønsted acid sites in the zeolite mordenite," *J. Phys. Chem. C*, vol. 118, no. 41, pp. 23918–23929, 2014, doi: 10.1021/jp5086334.
- [22] K. Suzuki, N. Katada, and M. Niwa, "Detection and quantitative measurements of four kinds of OH in HY zeolite," *J. Phys. Chem. C*, vol. 111, no. 2, pp. 894–900, Apr. 2007, doi: 10.1021/jp065054v.
- [23] K. D. Nugrahaningtyas, Y. Hidayat, Patiha, N. Prihastuti, B. Yelvi, and R. U. N. Kalimah, "Synthesis of the Supported Catalysts by Co- Impregnation and Sequential Impregnation Methods," *Mater. Sci. Eng.*, vol. 176, no. 1, pp. 12–24, 2017, doi: 10.1088/1757-899X/176/1/012024.
- [24] W. Trisunaryanti, T. Triyono, and D. F. A, "Preparation OF Ni-Mo / Mordenite Catalysts Under The variation Of Mo / Ni Ratio and Their Characterizations For Stearic Acid Conversion," *Indo. J. Chem*, vol. 3, no. 2, pp. 80–90, 2003.